

# New Applications of the Image Grand Tour

Jürgen Symanzik  
Utah State University, Department of Mathematics and Statistics  
3900 Old Main Hill, Logan, UT 84322-3900  
e-mail: [symanzik@math.usu.edu](mailto:symanzik@math.usu.edu)

Edward J. Wegman  
George Mason University, Center for Computational Statistics  
Fairfax, VA 22030-4444  
e-mail: [ewegman@galaxy.gmu.edu](mailto:ewegman@galaxy.gmu.edu)

Amy J. Braverman  
Jet Propulsion Laboratory, 4800 Oak Grove Drive  
Pasadena, CA 91109-8099  
e-mail: [amy.braverman@jpl.nasa.gov](mailto:amy.braverman@jpl.nasa.gov)

Qiang Luo  
RealNetworks, Inc., PO Box 91123  
Seattle, WA 98111-9223  
e-mail: [qluo@real.com](mailto:qluo@real.com)

## Abstract

The image grand tour (IGT) is a method for visualizing multispectral images or multiple registered images. Such images can be described as having a multivariate pixel vector associated with each pixel. Examples are the RGB values of a photograph or the multiple spectral and infrared readings from remote sensing satellites. The image grand tour projects a linear combination of the pixel vectors into one-dimensional space (for each pixel) and then renders these projected values as a gray-scale image. An animation of the projected images is obtained by using different linear combinations of the pixel vectors. While the image grand tour was initially used to highlight mines in a minefield, this paper presents new applications of the image grand tour. We use the IGT to find hidden rock art in photographs from sites in state parks in Texas and to reveal features in satellite imagery from the Multi-angle Imaging SpectroRadiometer (MISR), one of the instruments aboard NASA's Earth Observing System satellite Terra.

## Keywords

Animation, Minefield, MISR, Multi-angle Imaging SpectroRadiometer, Multispectral Images, Petroglyphs, Pictographs, Projection, Rock Art, Visualization.

## 1. Introduction

The grand tour of a multidimensional data set is a visualization technique for examining structure of high dimensional data using dynamic graphics. The idea, introduced in Asimov (1985) and Buja and Asimov (1986), is to capture, in some sense, the popular meaning of grand tour, that is, to look at a subject from all possible angles. In a data analytic setting, these authors propose projecting a  $d$ -dimensional data set into a dense set of the possible two-dimensional planes. If the sequence of projections is smooth, the visual impression is that the data points move in a continuous fashion from frame to frame of a movie. The object of the data analyst is to look for unusual

configurations of the data, configurations that may reflect some structure. The grand tour, in this sense, shares a common objective with the projection pursuit techniques. The added motion associated with the grand tour literally adds another dimension, the time dimension, which many data analysts find very helpful.

Wegman (1992) discussed a form of the grand tour for general  $k$ -dimensional space,  $k \leq d$ . The algorithms for computing a grand tour are relatively computationally intensive. Wegman and Shen (1993) discussed an approximate one- and two-dimensional grand tour algorithm that was much more computationally efficient than the Asimov *winding* algorithm. That algorithm was motivated in part by a discussion of the Andrews multidimensional data plot, which can also be regarded as a highly restricted tour.

The idea of the image grand tour (IGT) evolved from an initial application of one-dimensional tours to image data. Multiple registered images can be regarded as a multidimensional image in which each pixel location has a vector attached to it. Indeed, ordinary red, green, and blue (RGB) color images are vector-valued images. The basic idea of the image tour is to apply the same one-dimensional grand tour to each vector for all pixel locations in an image. This combines the vectors into a scalar function of time which can be rendered in as a time-varying gray-scale image. The Wegman and Shen (1993) algorithm generalizes easily to two dimensions, so that an alternate approach to the image grand tour is to project the multidimensional vector into two dimensions and render the image as a false color image with two complimentary colors such as red and cyan. The initial discussion of the image grand tour was given by Wegman et al. (1998).

Currently, the image grand tour software, written in C++ by one of us (QL), is available for Silicon Graphics (SGI) workstations. To obtain a fast rendering rate of large images, the software intensively uses SGI hardware features such as the  $\alpha$ -channel hardware. The reader may contact any of the authors to obtain a copy of the SGI version of the software. There is also a MATLAB version written by Wendy Martinez.

To use a simple photograph, such as those from Section 4, the image must be stored in binary format. This can be done by saving any image format (such as .gif, .tiff, or .jpg) as *IRIS RGB* using image processing software such as *xv* on an SGI workstation. The UNIX command *tobin* creates the required binary format (*tobin photo.rgb photo.bin*). The IGT software can then be started and an info (.i) file can be loaded. Required information for the info file are the width and height of the image, its depth (3 for a simple photograph, up to 36 for the images from Section 3), the number of channels (typically 1), and the number of files (1, if this file contains all partial images, or more, if the partial images are stored in separate files). A list of files that contain the partial images follows at the end. Below is an example of an .i file for a photograph:

```
#IMAGE SEQUENCE
135 //width
182 //height
3 //depth
1 //channels
1 //number of files
photo.bin
```

In this paper we will focus on three different examples where the IGT can be applied. In Section 2, we revisit the original minefield example from Wegman et al. (1998). In Section 3, we discuss how the IGT helped to detect features in satellite imagery from the Multi-angle Imaging SpectroRadiometer (MISR) instruments aboard NASA's Earth Observing System satellite Terra. In Section 4, we discuss how the IGT has been used to detect hidden rock art in photographs. We finish with a discussion in Section 5.

## 2. Application 1: Minefields

Consider a class of image analysis problems in which the analyst has a set of registered images. The initial example that originally motivated the idea of the IGT was multispectral imagery of minefields. In this application a suspected minefield was photographed in six spectral bands ranging from infrared to ultraviolet. We desire to locate mines in this field by combining the images in a mathematically appropriate manner. It is known that mines can be laid proud or slightly buried. Buried mines will stress vegetation hence alter infrared characteristics. Proud mines will absorb heat and re-radiate infrared. Decoy mines, generally hollow, will have different heat absorption characteristics. Rocks and other debris may have ultraviolet radiation patterns. It is fairly well known that using these multispectral images, one can distinguish among mines and other objects even if the resolution of the image is not sufficient to visually identify the objects. Even more interesting, as we shall demonstrate, it is possible to use our methodology to identify mine objects even if they do not appear visually distinct in any of the individual images.

Algorithmically for the one-dimensional tour, we desire to have a continuous vector-valued function  $a(t)$ , which is a unit vector and sweeps through all possible directions. The data vector  $x_{ij}$  is associated with pixel  $(i,j)$  so that  $y_{ijt}$  is the inner product of  $a(t)$  with  $x_{ij}$ . The continuity requirement assures that the transitions from frame to frame of the movie will be visually smooth allowing the eye to easily follow the images. The requirement to sweep through all possible directions assures that no projection of the multidimensional image will be overlooked. In this paper, we follow the Wegman and Shen (1993) algorithm, which is only a pseudo-grand tour. Functionally, however, we have found this to be quite adequate for our purposes. See Wegman et al. (1998) for details. The image will change as  $t$  increases.  $y_{ijt}$  is a scalar so that we have formed a series of orthonormal dynamically changing images. Each pixel location is a linear combination of the vector components at that location. For our mine detection application, the idea is that as we allow the time variable  $t$  to increase, some configurations of vector components will highlight the mines and suppress the other “noise” in the image.

In the minefield application, we have a six-dimensional image, i.e., one image each in six spectral bands. Figure 2.1 illustrates three of the six images of the minefield, those from filters 2, 4, and 6. Figure 2.2 shows a snapshot of the image grand tour. This selection was done by eye and was not a result of an optimization process. Figure 2.3 illustrates the entire window of the SGI-based application. The window in the bottom left corner illustrates the relative contribution of each of the six image components. [Movie 2.1](#) shows the process how the mines become visible and invisible, based on the relative contribution of the image components.

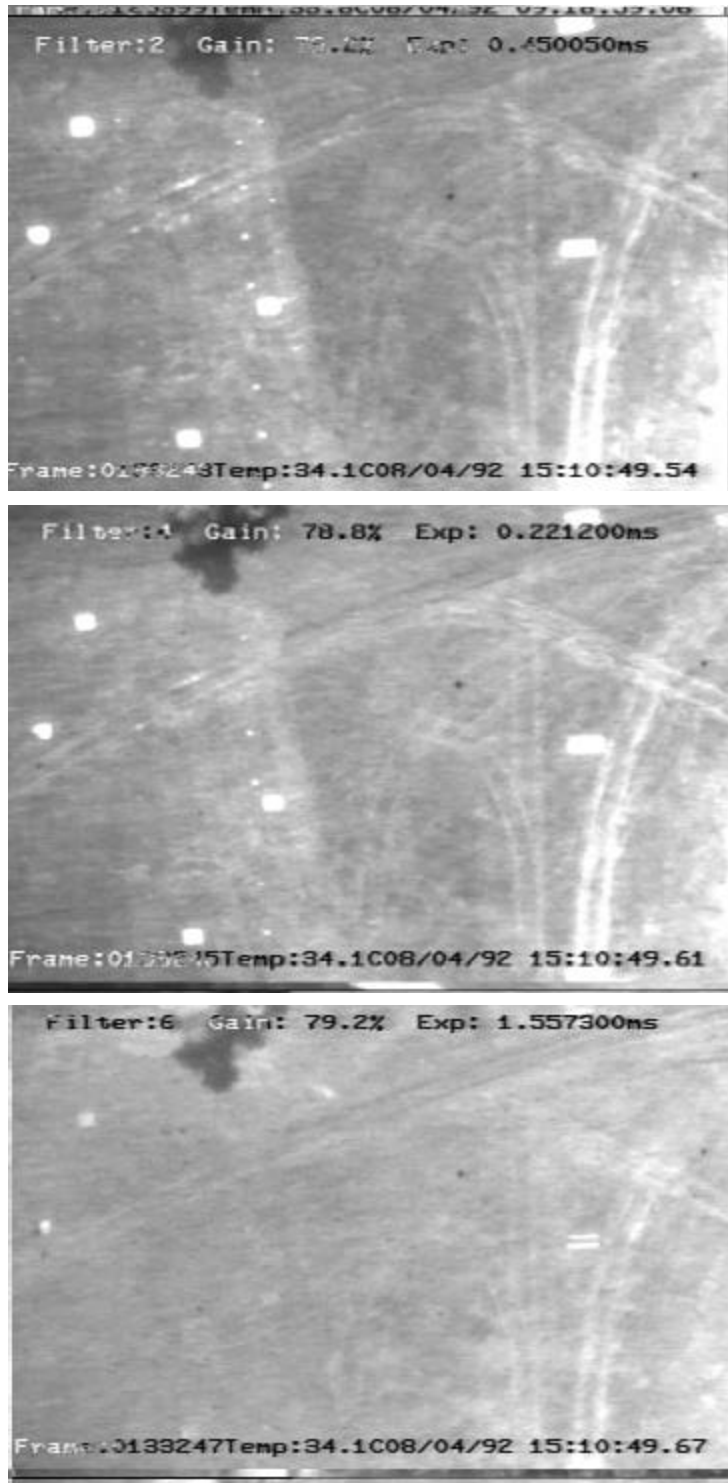


**Figure 2.1:** Three filtered images of the minefield. One set of mines is visible in the top image labeled Filter 2 as a near vertical row of white dots on the left-hand one-third of the image. Other mines are not conspicuous or even visible.



**Figure 2.2:** Image grand tour illustrating four rows of mines. The darkest row coincides with the row visible in Figure 2.1, Filter 2. Immediately to the left are two additional rows, the middle row somewhat staggered. There is also a less distinct row of mines to the right of the darkest row.



**Figure 2.3:** Window from the IGT minefield application. The display in the lower left hand corner gives relative intensities of contributions from each of the six filtered images.

### 3. Application 2: Multi-angle Imaging SpectroRadiometer (MISR) Images

Figure 3.1 depicts the NASA Earth Observing System satellite Terra spacecraft in polar orbit, with the MISR featured. The MISR is an array of nine cameras that look down at Earth at nine different angles along the flight path. The angles are 70.5 degrees off-nadir forward and aft (Df and Da cameras), 60 degrees forward and aft (Cf and Ca), 45 degrees forward and aft (Bf and Ba), 26.1 degrees forward and aft (Af and Aa), and 0 degrees (An; the nadir view). Each camera has four line arrays of charge couple device (CCD) detectors, and each detector sees a square ground footprint 275 meters on a side. 4 x 4 blocks of pixels are averaged to save space, so the effective pixel size is 1.1 km x 1.1 km. The cross-track field of view is about 300 km. Each line array is sensitive to a different spectral band: red (R), green (G), blue (B), and near-infrared (NIR). Thus, data produced by MISR can be conceptualized as a data set with 36 variables, i.e., 36 images at 9 angles x 4 wavelengths, and one row for each 1.1 km x 1.1 km pixel. Further details about MISR can be found at <http://www-misr.jpl.nasa.gov>.

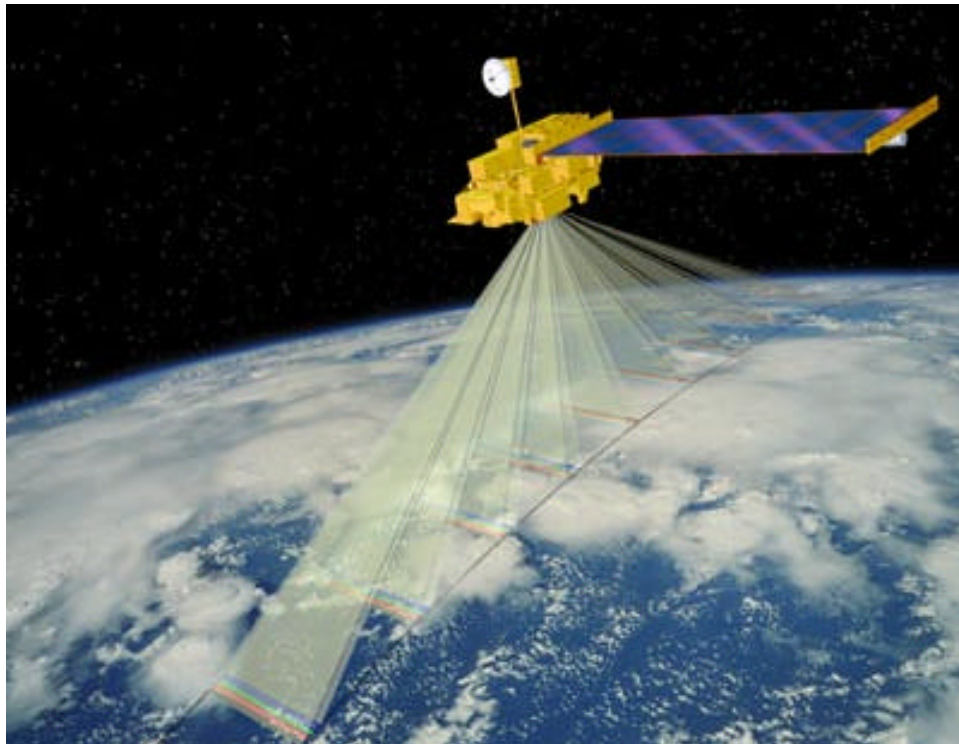


**Figure 3.1:** Terra spacecraft in polar orbit, with the MISR featured.

We would like to explore the 36-dimensional joint distribution of the MISR data and how it changes as we move spatially. In particular, this information may help us to classify geophysical characteristics of a scene that are otherwise indistinguishable. For example, Figure 3.2 is based on three of the 36 images for a scene over the north coast of Alaska including the Arctic National Wildlife Refuge (ANWR). This figure shows the nadir camera RGB composite acquired in June of 2001. Clouds, ice, land, and water are visible. There is considerable interest in distinguishing clouds from ice beneath it in order to study distributions of both clouds and ice in the polar regions. However, this is

sometimes difficult to do visually because clouds and ice have similar spectral signatures from the nadir view. At off-nadir view angles though, forward and back scattering of photons help distinguish ice of various textures, and paralax can be used to detect clouds since they are above the surface. Multiangle-multispectral data makes these identifications possible because different surfaces and atmospheric conditions cause photons to scatter differently as seen from different view angles. To make effective use of these data requires an exploratory technique that takes advantage of these features while retaining spatial relationships in the data. The IGT is such a technique.

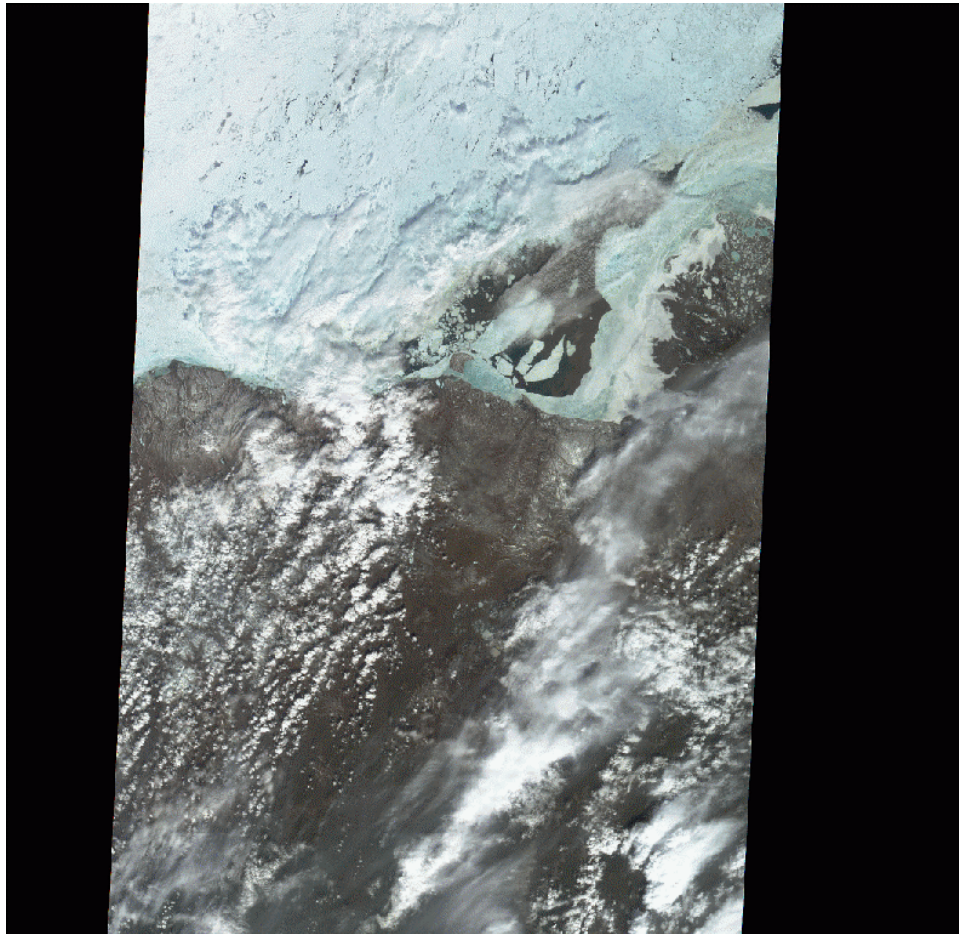


**Figure 3.2:** The nadir camera RGB composite, based on three of the 36 images, for a scene over the north coast of Alaska including the Arctic National Wildlife Refuge.

Consider two examples from the scene in Figure 3.2. Figure 3.3 is identical to Figure 3.2, with two areas marked in red boxes. First, consider the area on the left (the horizontally oriented rectangle that is wider than it is tall). [Movie 3.1](#) is an IGT animation of the 36 co-registered images of the ANWR scene. We notice that in frame 22 (at about 5 seconds) all 36 images receive equal weight (modulo the fact that it looks from the bar graph like a couple of them are zero-weighted) and that objects identifiable as clouds in Figure 3.2 appear blurred in movie frame 22. (Note that in Movie 3.1 the first 21 frames

are a static view of the same thing as frame 22. Frame 22 looks like approximately equal weight is given to each of the 36 images. At frame 22 the bar graph showing weights appears for the first time.) The blurring occurs because objects at higher altitude appear more displaced as the angle of view changes. When the images are averaged as in frame 22, this creates a smearing effect on the clouds because they are above the surface. The red rectangle on the left in Figure 3.3 shows blurring, indicating the presence of a cloud. Since the underlying scene is bright ice, this is difficult (if not impossible) to see in Figure 3.3.

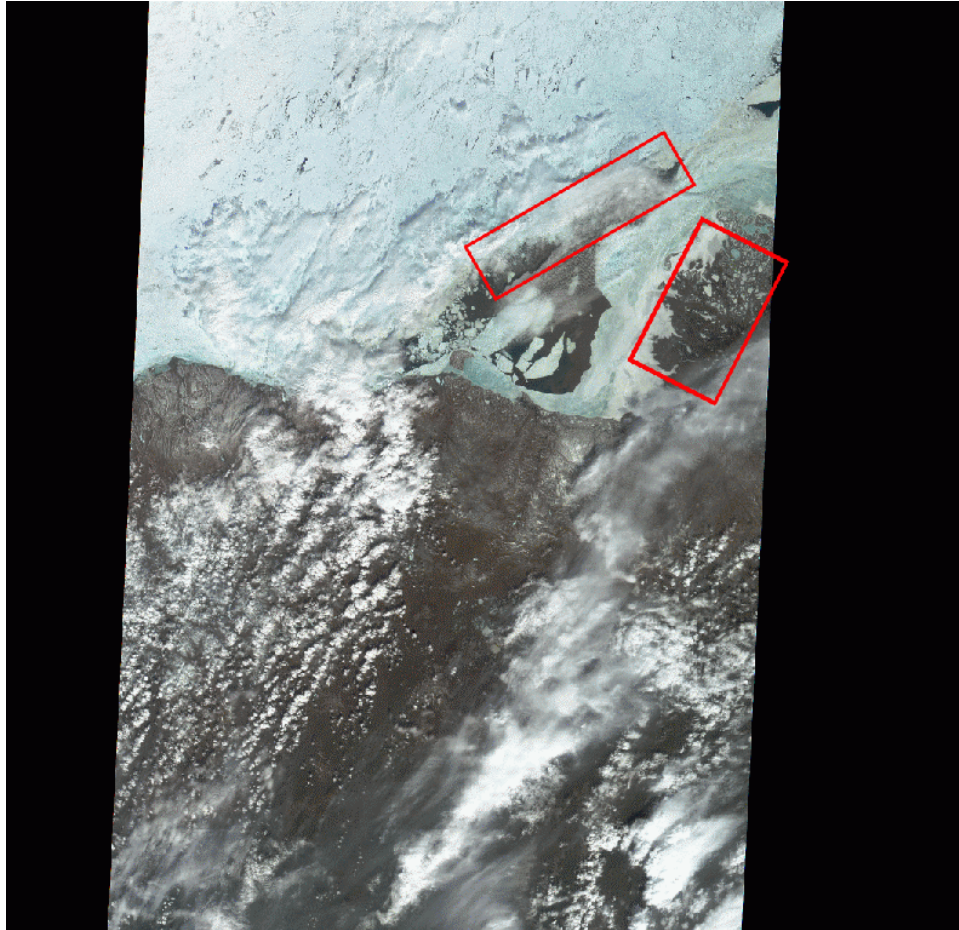


**Figure 3.3:** Same as Figure 3.2, with two regions being highlighted.

In the second example, the red box on the right in Figure 3.3 identifies a region that appears to be water with some ice and chunks of ice. At frame 48 (about 12 seconds) in Movie 3.1, we see a low-contrast scene showing ice cracks in an area that had appeared as open water in Figure 3.3. Most other features in the image are washed out, but the cracks show up as the contribution of the Bf camera increases (in the negative). Some of these cracks are barely visible in the Bf red image, but only after we know they are there. At frames 85-89 (about 21-22 seconds) more cracks and textures appear as the contribution of the A and B cameras increase. These cracks and textures are not obvious

in the individual static images. As the IGT proceeds, cracks and textures come and go, and we see that what we thought was dark water with ice chunks, must in fact be mostly translucent ice because of the cracking. At frames 95-99 (about 23-24 seconds) we see inhomogeneities in what originally appeared to be water. If we freeze the movie at some point, we note that these inhomogeneities are difficult to see. The fact that the graphic is dynamic (the textures come and go) is what calls attention to them. At frame 123 (about 30 seconds) a claw-like structure is visible near the left edge of the red box about half way up. This is obvious in frame 123, which is a mixture of B and C views, but not in any other single, original view. It is only the combination shown in frame 123 that reveals this structure.

In summary, combinations of the 36 images show things that cannot be seen or are very difficult to see in any of the original images, and continuous animation is key to spotting them. The fact that features smoothly and continuously come in and go out of view allows our brain to identify them in the same way as connecting dots in a plot of symbols does in a graph. (Before we connect the dots, they are just a bunch of dots. After we have connected them, we see a shape.) Finally, the effect of viewing linear combinations of images using animation is more than the sum of its parts. The combination of the two visualization techniques (i.e., blending and animation) embodied by the IGT does more than either could alone.

#### **4. Application 3: Rock Art**

Our final application deals with painted rock art images from the American Southwest. Rock art in the Southwest may extend back eleven thousand years when Paleo-Indians hunted now extinct animals such as mammoths. Within the archaeological literature, the term *pictograph* relates to figures painted on rock, while the term *petroglyph* relates to the forms pecked, incised, or ground into a rock surface. *Rock art* includes both of these terms (Hirschmann and Thybony, 1994).

In addition to natural causes such as wind, water, and erosion that can destroy rock art, vandalism is another factor. Gunfire, the carving of names and initials, and even touching a drawing by hand (not realizing that hand oils may have a damaging effect) can all lead to the destruction of pictographs and petroglyphs. While attempts are made to preserve images at least as watercolor renditions (Kirkland and Newcomb, 1967) or in photographs (Hirschmann and Thybony, 1994), unique rock art may have been lost before they could be documented.

Successful attempts to recover lost rock art images exist, e.g., the digital image enhancement technique developed by Mark and Billo (2002). Additional details on their work can be found at <http://www.infomagic.net/~rockart/>.

In this section we see how the IGT can be used to recover hidden pictographs. As examples, we work with two photographs from the Hueco Tanks State Historical Park east of El Paso, Texas, provided by Mark and Billo. More details on the Hueco Tanks site, paintings, and photographs are featured in Kirkland and Newcomb (1967), Chapter 8, and Hirschmann and Thybony, (1994), pages 14-17, respectively. Figure 4.1 and Figure 4.2 each show the original photograph (left image) and the digital reconstruction by Mark and Billo (right image). It appears as if the pictograph figure displayed in Figure 4.1 relates to the “black-outlined figure of a woman”, shown in Plate 147, 24-B, page 196, in Kirkland and Newcomb (1967).

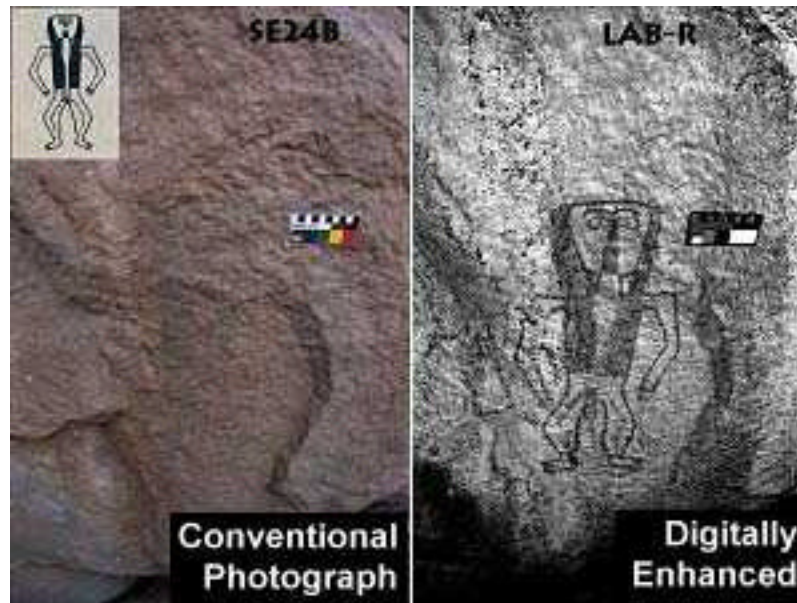


**Figure 4.1:** Faded pictograph image (left) and digitally enhanced image by Mark and Billo (right).

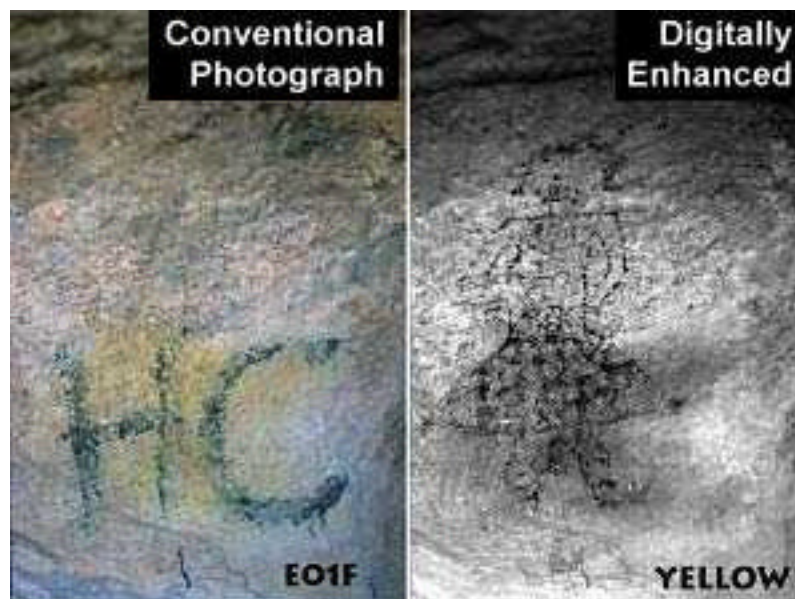


**Figure 4.2:** Pictograph image with spray-paint vandalism (left) and digitally enhanced image by Mark and Billo (right).

To use a photograph for the IGT software, we broke down each photograph into its red, green, and blue component, and stored these components as separate grayscale images (as outlined in Section 1). Thus, in contrast to the 36-dimensional data in the MISR application, we only have three-dimensional data in the rock art application. Figure 4.3 and Figure 4.4 show the reconstruction of the original images as obtained through the IGT software. Depending on screen resolution (or printout quality), it may be hard to see the painted rock art figures in Figure 4.3, Figure 4.4, and [Movie 4.1](#). This is due to the fact that the blended images result in relatively low-contrast grayscale images. The small inlays in Figure 4.3 and Figure 4.4 show further enhancements of the painted figures. The image processing software *xv* was used on an SGI workstation to enhance the contrast of these small images. [Movie 4.1](#) shows how the painted figure from Figure 4.3 becomes visible and invisible again based on the relative contribution of each of the three image components. The painted figure is best seen in this movie when the contribution of each of the three image components is similar to that displayed in Figure 4.3.

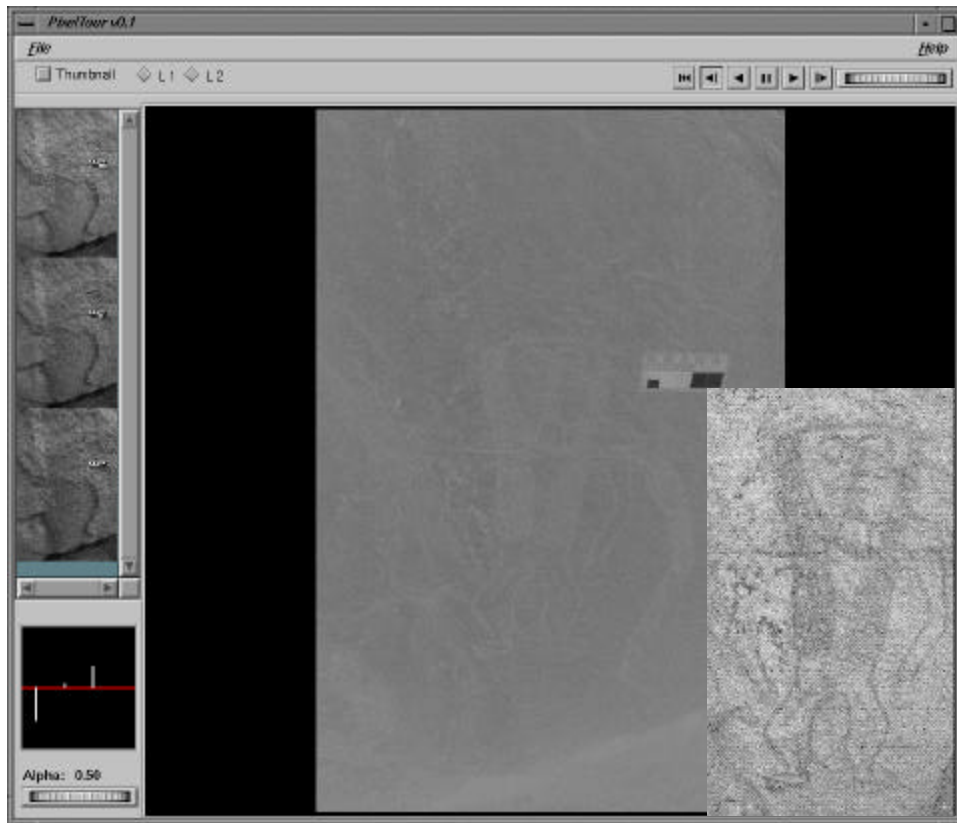


**Figure 4.3:** Reconstruction of the image from Figure 4.1 using the IGT.

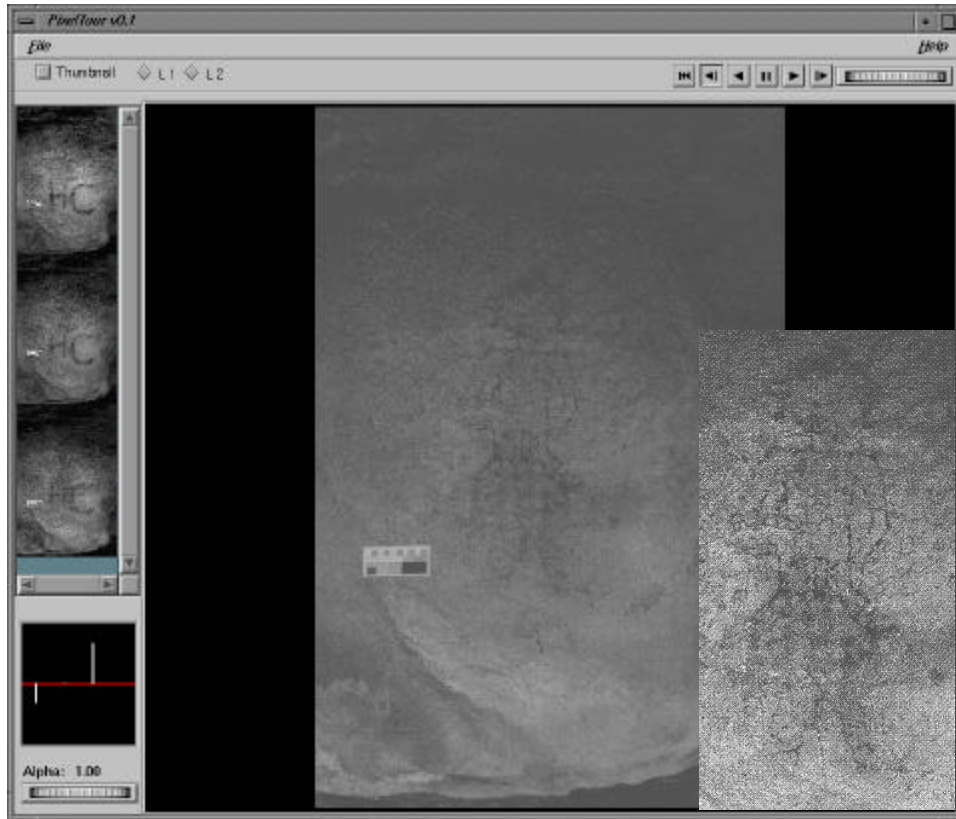


**Figure 4.4:** Reconstruction of the image from Figure 4.2 using the IGT.

## 5. Discussion

In this paper we have seen three different applications of the image grand tour: minefields, remotely sensed MISR data, and rock art photographs. The number of individual images that makes up a view varies between three (rock art) and thirty-six (MISR). The IGT is most effective when it is used interactively. Often, animation helps to detect features that are not visible at all or only very difficult to see in any static snapshot of the IGT. One of the big advantages of the IGT is that it can be used immediately without any further programming for quite different applications, with results ranging from astonishing (such as for the minefields and MISR) to fair (pictographs). In the rock art case, it is not too surprising that image enhancement techniques particularly developed for such types of images provide better results than the general-purpose IGT.

The results we obtained for the three different applications presented in this paper merit further development of the IGT software. One of its current main restrictions is that a reasonably fast version is only available on high-end SGI workstations. The MATLAB version of the IGT software for PCs is much slower and is restricted to less complex images. At this point, even the SGI version of the IGT is still limited in its functionality. One desirable feature of the software would be the ability to manually adjust or fix the contribution of one layer of the image towards the overall image. Also, a manual rearrangement of the order of the layers would help to shift layers that appear to

be more important than the others towards the top of the display for better visibility. Finally, one might discuss an extension of the IGT software towards colored composed images rather than rendering everything in grayscale.

### **Acknowledgments**

Thanks are due to Robert Mark and Evelyn Billo, Rupestrian CyberServices, for their helpful comments on rock art and for providing the original pictograph photographs as well as their image enhancements in Section 4. The work of the second author, EJW, was completed under the sponsorship of the Air Force Office of Scientific Research under the contract F49620-01-1-0274 and the Defense Advanced Research Projects Agency through cooperative agreement 8105-48267 with Johns Hopkins University.

### **References**

Asimov, D. (1985), "The Grand Tour: A Tool for Viewing Multidimensional Data," *SIAM Journal on Scientific and Statistical Computing* 6(1), 128-143.

Buja, B., and Asimov, D. (1986), "Grand Tour Methods: An Outline," in: Allen, D. M. (Ed.), *Computer Science and Statistics: Proceedings of the Seventeenth Symposium on the Interface*, Elsevier Science Publishers B.V. (North-Holland): Amsterdam, 63-67.

Hirschmann, F. (Photography), and Thybony, S. (Text) (1994), *Rock Art of the American Southwest*, Graphic Arts Center Publishing: Portland, OR, softbound edition 1999.

Kirkland, F. (Paintings), and Newcomb, Jr., W. W. (Text) (1967), *The Rock Art of Texas Indians*, The University of Texas Press: Austin, TX, reissued 1996.

Mark, R. K., and Billo, E. (2002), "Application of Digital Image Enhancement in Rock Art Recording," *American Indian Rock Art* 28, 121-128.

Wegman, E. J. (1992), "The Grand Tour in k-Dimensions," in: Page, C., and LePage, R. (Eds.), *Computing Science and Statistics: Proceedings of the 22nd Symposium on the Interface*, Springer-Verlag: New York, NY, 127-136.

Wegman, E. J., and Shen, J. (1993), "Three-Dimensional Andrews Plots and the Grand Tour," in: Tarter, M. E., and Lock, M. D. (Eds.), *Computing Science and Statistics: Proceedings of the 25th Symposium on the Interface*, Interface Foundation of North America: Fairfax Station, VA, 284-288.

Wegman, E. J., Poston, W. L., and Solka, J. L. (1998), "Image Grand Tour," in: *Automatic Target Recognition VIII - Proceedings of SPIE*, 3371, 286-294; republished in: Sadjadi, F. (Ed.), Vol. 6: *Automatic Target Recognition. The CD-ROM*, SPIE: Bellingham, WA, 1999.